



Long-term stability and sustainability evaluation for mode-locked fiber laser with graphene/PMMA saturable absorbers

K.Y. Lau^a, P.J. Ker^a, A.F. Abas^b, M.T. Alresheedi^b, M.A. Mahdi^{c,*}

^a Electronics Research Group, Institute of Power Engineering, Universiti Tenaga Nasional, 43000 Kajang, Selangor, Malaysia

^b Department of Electrical Engineering, College of Engineering, P.O. Box 800, King Saud University, Riyadh 11421, Saudi Arabia

^c Wireless and Photonic Networks Research Centre, Faculty of Engineering, Universiti Putra Malaysia, 43400 UPM Serdang, Selangor, Malaysia

ARTICLE INFO

Keywords:

Saturable absorber
Mode-locking
Fiber laser
Stability
Sustainability

ABSTRACT

A quality saturable absorber for the integration of a practical laser product with long-term stability and sustainability is of utmost importance to be delivered to end-users. Graphene/polymethyl-methacrylate saturable absorber is proposed with the advantage of gapless material characteristic for ultra-broadband wavelength operation. This saturable absorber possesses stability over 24-hour continuous mode-locked laser operation at 105.2 mW pump power, as well as sustainability over four consecutive observation weeks with the preservation of 670 fs pulse duration within the experimental period. Last but not least, the proposed saturable absorber shows excellent long-term stability and sustainability for the formulation of practical seed mode-locked fiber laser source.

1. Introduction

In recent years, the development of pulsed fiber laser in Q-switching and mode-locking mechanisms have exhibited great potential in governing the dynamics of pulse propagation in fiber optics. A Q-switched fiber laser generates the bursting of “giant pulse” when the Q-factor in the laser cavity is switched by a modulation technique such as saturable absorber (SA). For instance, a Q-switched fiber laser was demonstrated with graphene SA in wavelength switchable scheme [1] and a topological insulator SA in a large energy wavelength tunable Q-switching regime [2]. In addition, mode-locked fiber laser (MLFL) has exhibited great potential in governing the dynamics of pulse propagation in fiber optics. The MLFL is presented with pulse duration of several hundred femtosecond (fs) down to 70 fs as reported in [3]. A SA plays an important role to generate optical pulses in MLFL. In pulsed laser technology, the SA decreases the absorption of light with increasing light intensity. The saturable absorption is an optical phenomenon related to the excitation of atoms at ground state to excited state under high optical intensities, and insufficient decaying time is possessed by these atoms to revert into the ground state. Therefore, the ground state becomes depleted and the absorption is saturated. The losses can be temporarily reduced when saturable absorption takes place at high optical intensities. When the SA is implemented inside a laser cavity, the losses of the circulating pulses are lower than the laser gain at high optical intensities. Contrarily, the light with lower optical intensities which hits the SA experience higher losses than the laser gain. In the temporal evolution of MLFL, ultrashort pulse is generated at high optical

power when the laser gain is higher than the losses of the circulating pulse.

The SA possesses numerous advantages of a passive device over an active modulator in terms of simpler optical system integration and synchronization to generate optical pulses [4]. The evolution of SA materials has been demonstrated from semiconductor material [5], carbon nanotube (CNT) [6], graphene [7], topological insulator [8], transition metal dichalcogenides (TMD) [9,10], black phosphorus [11] and phosphorene quantum dot [12]. Research on absorber materials can be obtained from photovoltaic cell such as perovskite [13]. This material shows excellent absorption properties which are predicted as a potential SA candidate for MLFL generation. In 2018, Han Zhang et al. [14] proposed MXene ($\text{Ti}_3\text{C}_2\text{T}_x$) where T is O, F or OH, for the generation of mode-locked fiber laser at wavelengths of 1.07 μm and 1.56 μm . This material possesses graphene-like characteristics with excellent saturable absorption properties, which can be exploited for a new path in advanced photonics system. However, graphene has remained to be a convincing material due to its outstanding gapless material characteristic in generating pulse over broadband wavelength operation. This characteristic is absent in CNT with tube diameter dependent wavelength operation [15] and TMD with direct bandgap properties only in monolayer structure [16]. Therefore, graphene has been chosen as one of the promising SA candidates.

Several research works were conducted to study the fiber structure [17,18], dispersion effect [19], and gain medium in MLFL cavity [20], and even the implementation in random fiber laser for pulse

* Corresponding author.

E-mail address: kylau@uniten.edu.my (K.Y. Lau).

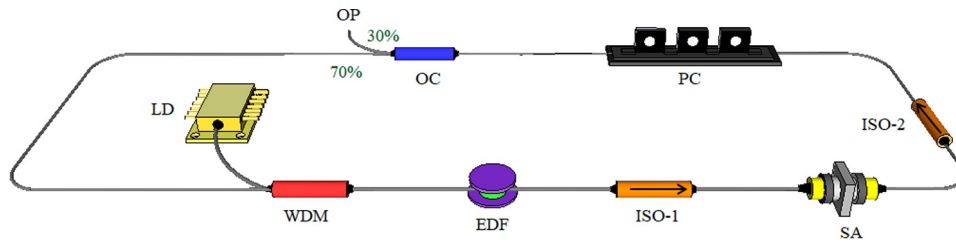


Fig. 1. Ring cavity MLFL incorporating graphene/PMMA-SA.

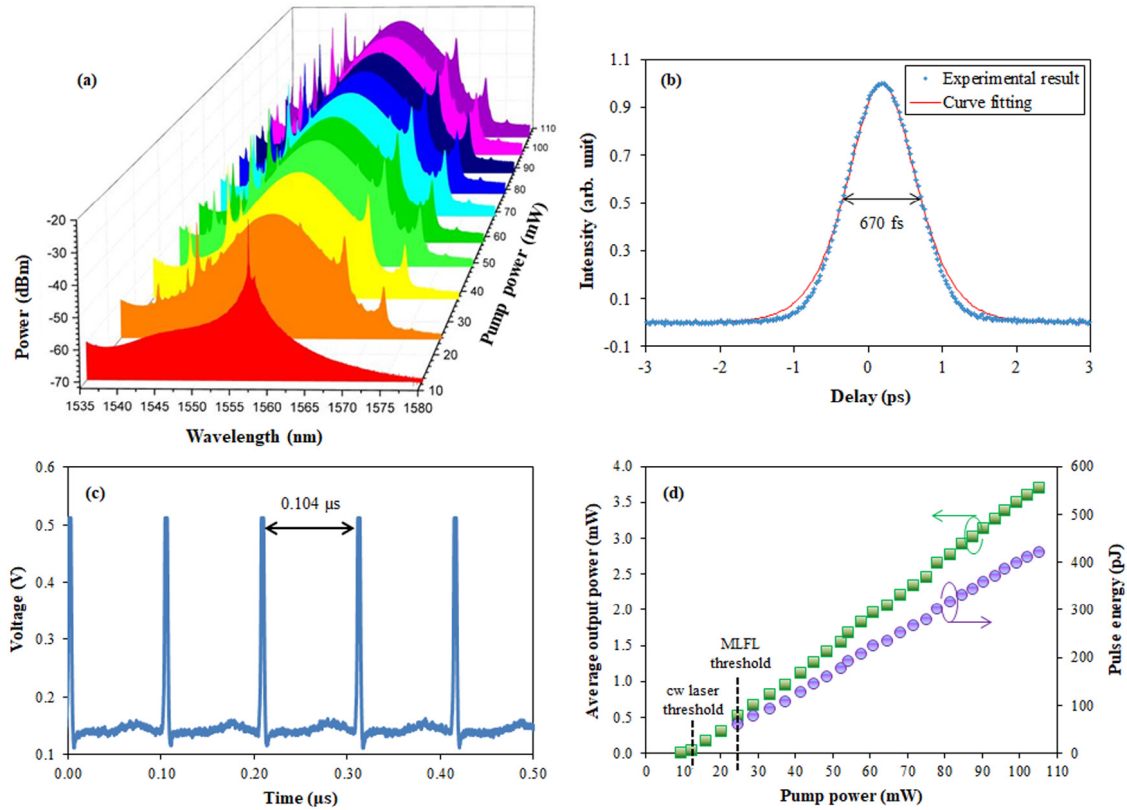


Fig. 2. (a) Optical spectrum, (b) autocorrelation trace, (c) oscilloscope trace, and (d) power development of MLFL.

generation [21] using graphene materials. Among the research works, the long-term evaluation of stability and sustainability of MLFL incorporating graphene SA, however, has remained elusive in the MLFL directories. S. Yamashita and associates [22] aware of this issue and evaluated the sustainability of CNT-based MLFL over seven observation days. This procedure is significant to authenticate the quality and robustness of the fabricated SA. Therefore, longer evaluation time is needed to ensure the stability and sustainability of SA before its practical implementation.

In this work, we evaluate the robustness of graphene/polymethylmethacrylate (graphene/PMMA) SA utilized in [23] by measuring its pulse performance over four weeks. The experimental findings show no signs of performance degradation which is crucial for practical implementation. This study demonstrates that the proposed graphene/PMMA SA is one of the suitable candidates for stable ultrashort pulse lasers.

2. Fiber laser experimental setup

Fig. 1 illustrates the schematic diagram of MLFL cavity. A 980 nm laser diode (LD) was used to pump 5 m erbium-doped fiber (EDF) via a 980/1550 wavelength division multiplexer (WDM). The EDF has a signal absorption coefficient of 3.5 dB/m at 1530 nm and a dispersion

coefficient of -18 ps/nm/km at 1550 nm. An isolator (ISO-1) was spliced with the EDF to force a unidirectional signal propagation of the laser cavity. The sandwiched-structure graphene SA experienced optical losses from the pigtail connector and the Fresnel reflection of the flat-angle pigtails. In order to minimize multiple reflections in the cavity originated from this specific joint, another isolator (ISO-2) was employed with the same direction as the ISO-1. A polarization controller (PC) was used to manipulate the polarization states in the non-polarization maintaining laser cavity. Next, the PC was connected to an optical coupler (OC) to channel out 30% of MLFL signal for further analysis. Last but not least, the remaining 70% of MLFL signal was reverted into the 1550 nm port of the WDM to complete the laser cavity.

3. Basic characteristic of MLFL

Fig. 2(a) shows the optical spectrum of the MLFL measured with 0.02 nm resolution of optical spectrum analyzer. The continuous wave (CW) laser and MLFL were generated at pump powers of 12.3 mW and 24.5 mW, respectively. The MLFL pump power threshold was influenced by the laser cavity loss and saturation intensity, a parameter to saturate the absorption of graphene/PMMA-SA at 3.4 MW/cm² in [23]. Fig. 2(b) depicts the autocorrelation trace of the MLFL at maximum pump power.

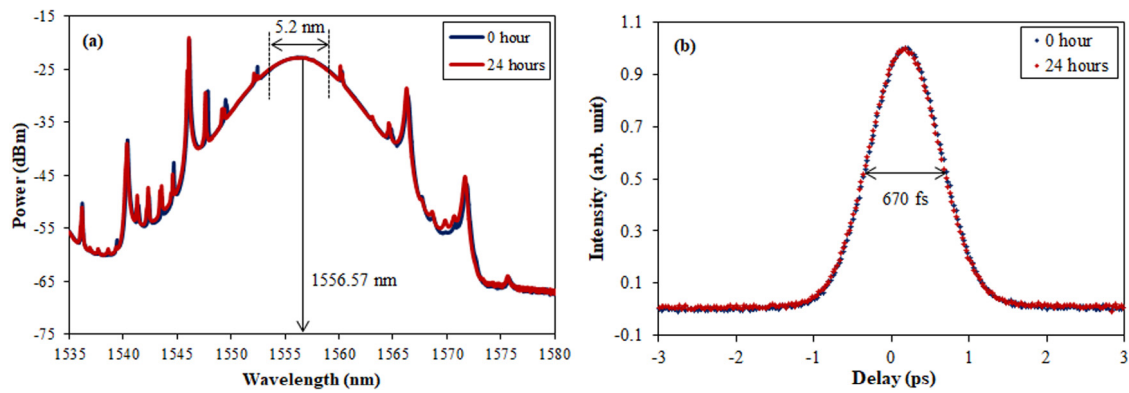


Fig. 3. Stability evaluation of (a) optical spectrum and (b) autocorrelation trace for MLFL over 24 h.

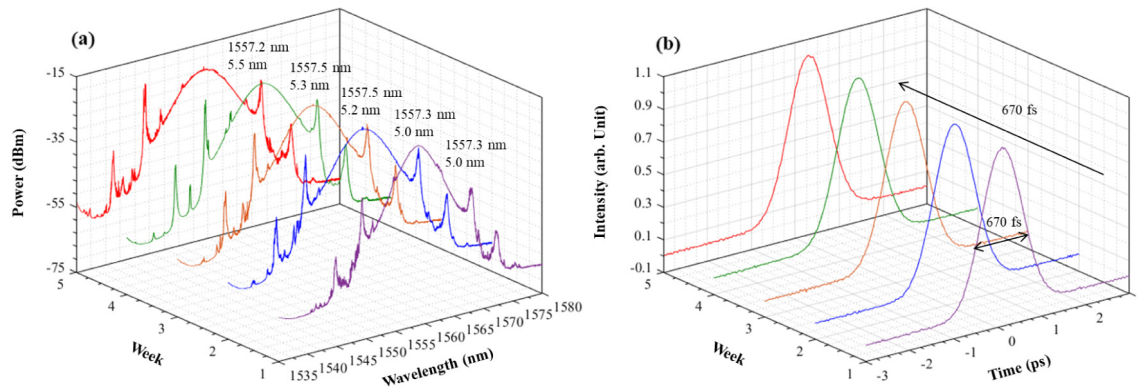


Fig. 4. Sustainability evaluation of (a) optical spectrum and (b) autocorrelation trace of MLFL for four consecutive observation weeks.

The autocorrelation pulse width was measured at 1.03 ps. The curve fitting was performed with secant hyperbolic pulse shaping profile. The pulse width at full width half maximum point of 670 fs was attained with decorrelation factor of 0.648 from autocorrelation pulse width. The time-bandwidth product for this Fourier-transform limited MLFL pulse was thus calculated as 0.426, indicating that the pulse was slightly chirped. Fig. 2(c) shows the oscilloscope trace of MLFL at maximum pump power. The fundamental pulse was measured with a response time of 0.104 μ s or a pulse repetition rate of 9.65 MHz. The pulse repetition rate is in conjunction with the manually measured total cavity length of 21.3 m. Based on the 5 m EDF, 1 m Hi-1060 fiber for signal wavelength coupling purpose, and 15.3 m single-mode fiber, the net group velocity dispersion was calculated as -0.17 ps². The net anomalous dispersion of the laser cavity substantiates the multiple Kelly's sidebands in the optical spectrum. The power development of the MLFL is portrayed in Fig. 2(d). The CW laser and MLFL thresholds are in agreement with Fig. 2(a) at 12.3 mW and 24.5 mW, respectively. The average output power increases from 44.6 μ W to 3.7 mW as the pump power varies from 12.3 mW to 105.2 mW. The pulse energy was deduced by dividing the average output power by the pulse repetition rate. At the maximum pump power of 105.2 mW, the pulse energy was calculated as 420.8 pJ.

4. Stability evaluation of MLFL

Two important measurements of MLFL; optical spectrum [Fig. 3(a)] and autocorrelation trace [Fig. 3(b)] were plotted at 105.2 mW maximum pump power for stability evaluation purpose. At the beginning of the stability evaluation test, the spectral bandwidth of MLFL was 5.22 nm centered at the wavelength of 1556.57 nm. Referring to Fig. 3(a), the spectral bandwidth and center wavelength of MLFL are recorded at 5.17 nm and 1556.57 nm, respectively after 24 h of continuous MLFL operation. The negligibly small deviation in spectral bandwidth concludes the high stability of the proposed graphene/PMMA-SA in MLFL cavity. This clarification is enhanced by stable pulse width

preserved at 670 fs after 24 h of continuous MLFL operation, as shown in Fig. 3(b).

5. Sustainability evaluation of MLFL

Apart from stability evaluation, sustainability evaluation for MLFL was conducted over four consecutive observation weeks. The measurement was taken at a constant pump power of 105.2 mW. Based on the experimental findings, the graphene/PMMA-SA shows excellent sustainability for MLFL generation. The minor difference in the spectral shape in Fig. 4(a) is attributed to the fluctuations of polarization states since the laser cavity is composed of non-polarization maintaining fiber. In addition, this phenomenon could be due to the polarization rotation in vector soliton which produces a new set of weak sidebands as discussed in [24,25]. These weak sidebands are formed by the constructive interference between the dispersive waves emitted by the solitons with the polarization states periodically rotate in the laser cavity. The center wavelength and spectral bandwidth were measured ranging from 1557.2 to 1557.5 nm and from 5.0 nm to 5.5 nm, respectively, within the observation time. Despite the minor deviation in the center wavelength and spectral bandwidth, the pulse duration was maintained at 670 fs as presented in Fig. 4(b). Therefore, the proposed graphene/PMMA-SA is practical for the integration of seed MLFL source due to its high stability and sustainability.

6. Conclusion

In conclusion, we have successfully demonstrated a study on the stability and sustainability of optical pulse generated by graphene/PMMA SA in erbium-doped fiber laser. The SA was made by placing the graphene/PMMA in between two fiber ferrules. The fabricated SA has been tested for 24 h continuous operation and the measured optical

pulse duration maintained at 670 fs. In addition, the quality of optical pulse was also monitored over four weeks and the pulse duration remained constant. This study provides the information for our proposed graphene/PMMA SA in terms of its stability and sustainability. Based on the experimental findings, it is suitable for practical incorporation in MLFL to be utilized as a seed source.

Acknowledgments

The authors extend their appreciation to the International Scientific Partnership Program ISPP at King Saud University, Saudi Arabia for funding this research work through ISPP#0106. This work is also partly supported by Ministry of Education Malaysia under research grant FRGS/1/2017/TK04/UPM/01/2.

References

- [1] Z.T. Wang, Y. Chen, C.J. Zhao, H. Zhang, S.C. Wen, Switchable dual-wavelength synchronously Q-switched erbium-doped fiber laser based on graphene saturable absorber, *IEEE Photonics J.* 4 (3) (2012) 869–876.
- [2] Y. Chen, C. Zhao, S. Chen, J. Du, P. Tang, G. Jiang, H. Zhang, S. Wen, D. Tang, Large energy, wavelength widely tunable, topological insulator Q-switched erbium-doped fiber laser, *IEEE J. Sel. Top. Quantum Electron.* 20 (5) (2014) 0900508.
- [3] W. Liu, L. Pang, H. Han, W. Tian, H. Chen, M. Lei, P. Yan, Z. Wei, 70-fs mode-locked erbium-doped fiber laser with topological insulators, *Sci. Rep.* 6 (2016) 19997.
- [4] A. Martinez, K. Fuse, B. Xu, S. Yamashita, Optical deposition of graphene and carbon nanotubes in a fiber ferrule for passive mode-locked lasing, *Opt. Express* 18 (22) (2010) 23054–23061.
- [5] L. Zhang, J. Zhou, Z. Wang, X. Gu, Y. Feng, SESAM mode-locked, environmentally stable, and compact dissipative soliton fiber laser, *IEEE Photonics Technol. Lett.* 26 (13) (2014) 1314–1316.
- [6] K.Y. Lau, E.K. Ng, M.H. Abu Bakar, A.F. Abas, M.T. Alresheedi, Z. Yusoff, M.A. Mahdi, Low threshold L-band mode-locked ultrafast fiber laser assisted by microfiber-based carbon nanotube saturable absorber, *Opt. Commun.* 413 (2018) 249–254.
- [7] Z. Sun, T. Hasan, F. Torrisi, D. Popa, G. Privitera, F. Wang, F. Bonaccorso, D.M. Basko, A.C. Ferrari, Graphene mode-locked ultrafast laser, *ACS Nano* 4 (2) (2010) 803–810.
- [8] Y.I. Jhon, J. Lee, Y.M. Jhon, J.H. Lee, Topological insulators for mode-locking of 2- μ m fiber lasers, *IEEE J. Sel. Top. Quantum Electron.* 24 (5) (2018) 1–8.
- [9] B. Guo, S. Li, Y.-X. Fan, P. Wang, Versatile soliton emission from a WS₂ mode-locked fiber laser, *Opt. Commun.* 406 (2018) 66–71.
- [10] M. Liu, W. Liu, L. Pang, H. Teng, S. Fang, Z. Wei, Ultrashort pulse generation in mode-locked erbium-doped fiber lasers with tungsten disulfide saturable absorber, *Opt. Commun.* 406 (2018) 72–75.
- [11] X. Sun, H. Nie, J. He, R. Zhao, X. Su, Y. Wang, B. Zhang, R. Wang, K. Yang, Passively mode-locked 1.34 μ m bulk laser based on few-layer black phosphorus saturable absorber, *Opt. Express* 25 (17) (2017) 20025–20032.
- [12] J. Du, M. Zhang, Z. Guo, J. Chen, X. Zhu, G. Hu, P. Peng, Z. Zheng, H. Zhang, Phosphorene quantum dot saturable absorbers for ultrafast fiber lasers, *Sci. Rep.* 7 (2017) 42357.
- [13] N.-G. Park, Perovskite solar cells: an emerging photovoltaic technology, *Mater. Today* 18 (2) (2015) 65–72.
- [14] X. Jiang, S. Liu, W. Liang, S. Luo, Z. He, Y. Ge, H. Wang, R. Cao, F. Zhang, Q. Wen, J. Li, Q. Bao, D. Fan, H. Zhang, Broadband nonlinear photonics in few-layer MXene Ti₃C₂T_x (T = F, O, or OH), *Laser Photonics Rev.* 12 (2018) 1700229.
- [15] C.L. Cheung, A. Kurtz, H. Park, C.M. Lieber, Diameter-controlled synthesis of carbon nanotubes, *J. Phys. Chem. B* 106 (10) (2002) 2429–2433.
- [16] M.M. Ugeda, A.J. Bradley, S.F. Shi, H. Felipe, Y. Zhang, D.Y. Qiu, W. Ruan, S.K. Mo, Z. Hussain, Z.X. Shen, F. Wang, Giant bandgap renormalization and excitonic effects in a monolayer transition metal dichalcogenide semiconductor, *Nature Mater.* 13 (12) (2014) 1091.
- [17] Z. Wang, Y. Hou, Ultra-multiband absorption enhancement of graphene in a metal–dielectric-graphene sandwich structure covering terahertz to mid-infrared regime, *Opt. Express* 25 (16) (2017) 19185–19194.
- [18] W. Xin, Z.B. Liu, Q.W. Sheng, M. Feng, L.G. Huang, P. Wang, W.S. Jiang, F. Xing, Y.G. Liu, J.G. Tian, Flexible graphene saturable absorber on two-layer structure for tunable mode-locked soliton fiber laser, *Opt. Express* 22 (9) (2014) 10239–10247.
- [19] H. Zhang, D.Y. Tang, L.M. Zhao, Q.L. Bao, K.P. Loh, B. Lin, S.C. Tjin, Compact graphene mode-locked wavelength-tunable erbium-doped fiber lasers: from all anomalous dispersion to all normal dispersion, *Laser Phys. Lett.* 7 (8) (2010) 591.
- [20] J. Sotor, G. Sobon, J. Tarka, I. Pasternak, A. Krajewska, W. Strupinski, K.M. Abramski, Passive synchronization of erbium and thulium doped fiber mode-locked lasers enhanced by common graphene saturable absorber, *Opt. Express* 22 (5) (2014) 5536–5543.
- [21] B.C. Yao, Y.J. Rao, Z.N. Wang, Y. Wu, J.H. Zhou, H. Wu, M.Q. Fan, X.L. Cao, W.L. Zhang, Y.F. Chen, Y.R. Li, Graphene based widely-tunable and singly-polarized pulse generation with random fiber lasers, *Sci. Rep.* 5 (2015) 18526.
- [22] B. Xu, A. Martinez, S.Y. Set, C.S. Goh, S. Yamashita, A net normal dispersion all-fiber laser using a hybrid mode-locking mechanism, *Laser Phys. Lett.* 11 (2) (2014) 025101.
- [23] K.Y. Lau, M.H. Abu Bakar, F.D. Muhammad, A.A. Latif, M.F. Omar, Z. Yusoff, M.A. Mahdi, Dual-wavelength, mode-locked erbium-doped fiber laser employing a graphene/polymethyl-methacrylate saturable absorber, *Opt. Express* 26 (10) (2018) 12790–12800.
- [24] L.M. Zhao, D.Y. Tang, H. Zhang, X. Wu, Polarization rotation locking of vector solitons in a fiber ring laser, *Opt. Express* 16 (14) (2008) 10053–10058.
- [25] Y.F. Song, H. Zhang, D.Y. Tang, D.Y. Shen, Polarization rotation vector solitons in a graphene mode-locked fiber laser, *Opt. Express* 20 (24) (2012) 27283–27289.